A98-31467

ICAS-98-1,7,2

A Study of Self Induced Oscillatory Rolling Motion: Analytical and Experimental Results

G. Guglieri * F.B. Quagliotti †
Politecnico di Torino
Dipartimento di Ingegneria Aeronautica e Spaziale
Torino - Italy

Abstract

The paper deals with the study of an analytical model of wing rock, based on parameter identification of experimental data.
The experiments were performed in the Aeronautical Laboratory of Politecnico di Torino, in the D3M Low Speed Wind Tunnel, on a 80° delta wing. Free-to-roll tests have been used to determine build up and limit cycle characteristics of wing rock. Flow visualization techniques were also utilized in order to track vortex positions.
The characteristics of limit cycle (oscillation amplitude and frequency) were compared in detail with reference results obtained in other laboratories.
An analytical nonlinear model was derived. Parameters were identified by means of least squares approximation of experimental data with coherent initial conditions. The consistency of time histories, reproduced by numerical integration, was also analyzed.
This formulation correctly predicts stable limit cycles for a wide range of airspeeds, angles of attack and release roll angles.

Nomenclature

a_i	non dimensional coefficients
b	wing span
c	wing root chord
C_l	rolling moment coefficient (L/qSb)
f	oscillation frequency
I_{xx}	model inertia
k	reduced oscillation frequency (πfb/V)
L	rolling moment
q	dynamic pressure ($\rho V^2/2$)
S	model wing surface
S_{wt}	wind tunnel cross section
Re	Reynolds number (based on c)
t	time
$\hat{t}$	non dimensional time (t/t*)
t*	reference time (b/2V)
TPI	Politecnico di Torino
V	airspeed
α	angle of attack
β	angle of sideslip
ϕ	roll angle
ϕ_o	release roll angle
$\Delta\phi$	oscillation amplitude in roll
ρ	air density
$\dot{}$	time derivative
$\bar{}$	averaged data

Introduction

Wing rock is an oscillatory rolling motion of the aircraft with increasing amplitude up to a limit cycle. The final state is generally stable and characterized by both large roll attitudes and coupling with directional modes. Handling qualities are obviously compromised and the maneuvering capabilities degrade in terms of maximum achievable angle of attack. Moreover the presence of wing rock in the approach or landing phase can produce very serious consequences on the operational safety of the aircraft.

This phenomenon, arising from a nonlinear aerodynamic mechanism [1], has been documented in flight at high angle of attack, on configurations with slender forebodies and highly swept wing planforms combined with leading edge extensions. High speed civil transport and combat aircraft can fly in

*Assistant Professor, Member AIAA/AHS/AIDAA
†Associate Professor, Member AIAA/AIDAA

21st ICAS Congress
13-18 September 1998
Melbourne, Australia

conditions where this self-induced oscillatory rolling motion is observed.
The aerodynamic regime on these configurations is dominated by vortical flows. Evidence is given that, during wing rock oscillations, the normal position in the crossflow plane of vortex cores is affected by hysteresis. The roll angular velocity greatly influences both the pressure distribution on the wing surface and the roll damping. Furthermore, the vortex strength varies during the wing rock process. Free to roll and forced oscillation tests on slender delta wings indicated that wing rock build up is substantially promoted by roll damping decrease at high angles of attack.

The prediction and, consequently, the understanding of the physical mechanism of generation of wing rock is essential in order to design control systems able to suppress or alleviate this form of degraded stability.

The systematic approach to the study of wing rock is based on wind tunnel experimental investigation of roll dynamics for highly swept delta wing models [2, 3, 4, 5, 6, 7]. These simplified geometries exhibit stable limit cycles and correctly reproduce the dominant effect of primary wing vortices.

Differently, the analysis of complete aircraft roll dynamics is slightly more complicate, as the relevant aerodynamic interactions between forebody, lifting surfaces and empennages may complicate the understanding of the onset mechanism of wing rock.

In the present paper, the generation of wing rock is analyzed by means of wind tunnel experiments [11], that were carried out on a 80° delta wing model.
Flow visualizations were also performed and a correlation between vortex displacements and roll attitudes is derived.
An analytical model for the prediction of wing rock dynamics was validated. This nonlinear formulation is able to describe the most relevant aspects of the phenomenon.

Experimental Activity

Free-to-roll experiments were performed on a delta wing for $\alpha = 21° - 45°$, V = 15 m/s − 40 m/s, Re = 486000 − 1290000 and $\phi_o = 0° - 90°$.

The experimental tests were carried out in the D3M low speed wind tunnel at Politecnico di Torino. The test section is circular (3 m in diameter). The turbulence level is 0.3% at V = 50 m/s.

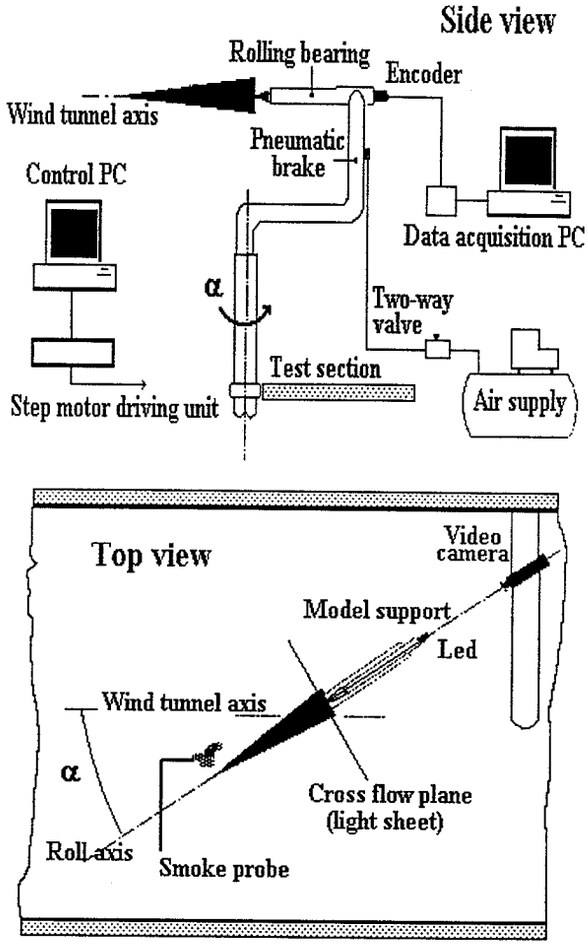

Figure 1: The experimental setup.

The model was a 80° delta wing with sharp leading and trailing edges, made in aluminum alloy. The dimensions are: root chord c = 479 mm, span b = 169 mm, thickness 12 mm, bevel angle 20°. The wing longitudinal body axis and the bearings axis coincide. The rotating system was statically balanced.

The C-shaped support (Fig. 1) was mounted on a vertical strut which was able to rotate so that the angle of attack could change while the model centroid remained at the center of the test section.

The model was connected to a horizontal shaft supported by rolling bearings. In order to minimize the friction of the angular transducer, the motion of the wing was measured by an optical encoder, linked with the rotating shaft using an elastic joint without backlash. This digital transducer was able to provide a resolution of 0.45°/bit.

A pneumatic brake was adopted to keep the wing in the initial angular position. During wind on

runs, a trigger signal was sent by the operator to the data acquisition unit and the model was released by a pneumatic cylinder fit inside of the vertical arm of the C-shaped support.

The digital signals generated by the encoder, which identify the sign, the increment and the zero crossing of ϕ(t), were conditioned by an electronic device consisting of an incremental counter and a 12 bit digital to analog converter. Both the analog output and the zero crossing trigger signal were multiplexed with a rate of 50 samples/s over a period of 45 s. The data acquisition system was based on a 12 bit analog to digital converter and an oscilloscope for the real time signal monitoring.

The amplitude and the oscillation frequency of the limit cycles were identified after the numerical elaboration of the time histories ϕ(t) with a spectral analyzer. The angular rates were evaluated numerically.

The rolling moment coefficient was evaluated considering that

$$C_l = \frac{I_{xx}}{qSb}\ddot{\phi} \qquad (1)$$

where $I_{xx} = 1.0117 \cdot 10^{-3}$ Kg m^2 is the rotational inertia. The coefficient C_l includes the effect of friction. A direct measurement of the static torque due to friction in wind off conditions confirmed that this contribution is negligible ($L = 4.5 \cdot 10^{-4}$ Nm).

In Ref. [8, 9] an extensive derivation of criteria for inertia similitude between different models, or model and aircraft, is given. These criteria state that similitude is ensured when the two configurations possess the same non dimensional ratio $I_{xx}/\rho b^5$. Hence, the non dimensional inertia for different models and aircraft is compared in Fig. 2. This analysis demonstrates that relevant scaling factors are required in order to compare in-flight wing rock with free to roll experiments. Similar factors apply for models with the same geometry tested in different wind tunnels.

The comparison of different reference model geometries and blockage factors S/S_{wt} is presented in Tab. .

The results presented (Fig. 3) are substantially similar to those given in Ref [4] by A.S. Arena and R.C. Nelson. The agreement with Ref [3] (Nguyen, Yip and Chambers) is limited to the lower angle of attack range ($\alpha \leq 35°$). Important differences are found among the majority of the experimental data and the oscillation amplitudes measured in Ref [2] by D. Levin and J. Katz. The maximum is shifted ($\Delta\alpha = -7°$) and the amplitude is reduced. The explanation of these discrepancies is the peculiar model geometry, which altered the vortex dynamics, due to the presence of a fuselage. As a matter of fact, even the onset of vortex breakdown was consistently anticipated ($\Delta\alpha = -10°$).

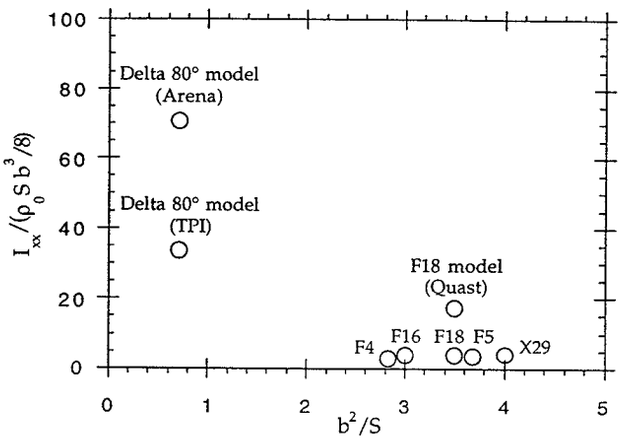

Figure 2: Wing aspect ratio b^2/S and rotational inertia I_{XX} for different models and aircraft.

Model	c [mm]	b [mm]	S/S_{wt}
Ref. [3]	1760	620	0.041
Ref. [2]	428	150	0.032
Ref. [4]	422	149	0.085
Ref. [7]	200	70	0.019
Ref. [11]	479	169	0.006

Table 1: The geometrical characteristics of several 80° delta wing models.

The comparisons performed for the oscillation frequency (Fig. 4) confirm the accordance with the measurements presented in Ref [4]. The trend of $k(\alpha)_{TPI}$ is coincident but shifted to higher values. This difference is a direct consequence of the different rotational inertia of the experimental apparatus adopted in Ref [4]. The experiences performed by A.S. Arena and R.C. Nelson establish that the oscillation frequency is proportional to $1/\sqrt{I_{xx}}$ and that the amplitude $\Delta\phi$ is not substantially changed by I_{xx}. Anyway, the inertial scaling of the results performs correctly, as confirmed by the second com-

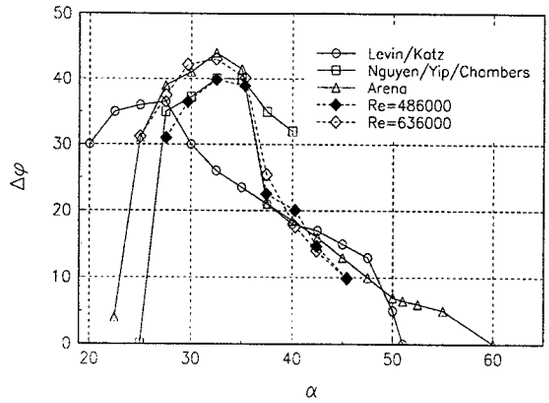

Figure 3: The experimental oscillation amplitude at different angles of attack.

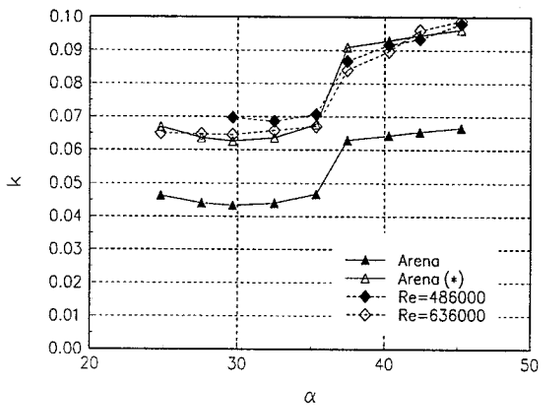

Figure 4: The experimental oscillation frequency at different angles of attack.

parison (k^*) presented in Fig. 4.

The onset of stable wing rock oscillations α_{ON} depends on airspeed. Some tests were performed reducing the angle of incidence during the oscillation of the model, in order to evaluate the lower limit α_{OFF} for the stability of the limit cycle (Tab. 2).

Some visualizations were also performed at V = 10 m/s with the aim of tracking the vortex dynamics in the crossflow plane. A smoke probe was positioned in front of the model apex (Fig. 1). The sheet of light was placed along the trailing edge (section at x/c = 1.0) and a video camera was aligned with the rotation axis, that was marked by

Re	α_{ON} [deg]	α_{OFF} [deg]
486000	27°	25°
636000	25°	23°
959000	25°	21°
1290000	25°	21°

Table 2: The lower stability boundaries of wing rock limit cycle.

a led. The images were digitized step after step so that the dynamic vortex core displacements could be accurately measured and reduced to the body axes frame.

The tracking of the primary vortex positions in the crossflow plane supports the validity of some experimental observations [4] concerning the explanation of the driving mechanism of wing rock.
The hysteresis of the normal coordinate z/b is dominant (Fig. 5), while only a marginal time lag is shown for the spanwise vortex core position y/b (Fig. 6).
During the limit cycle, the vortex cores move symmetrically on the two parts of the wing, so that $z_r(\hat{t}) = z_l(\hat{t} \pm \pi/k)$.
The reduction of the distance z/b between vortex core and wing upper surface generates a local increment of suction. The opposite is verified when the normal distance is increased. Therefore the term $(z_r - z_l)$ becomes an indicator of the differential lift acting on the rolling wing. The clockwise cyclic variation of this asymmetry parameter proves that both the dynamic displacement of the two primary vortices and the restoring aerodynamic moment are coupled.

The limit cycle presented in Fig. 5 - 6 is not affected by vortex breakdown. Hence, no direct relationship can be established between the onset of wing rock and the stability of the primary vortices. On the contrary, the magnitude of amplitude and frequency of the limit state is strongly coupled with this phenomenon, which was observed for $\alpha > 37°$. The sudden changes of the parameters $\Delta\phi$ and k for $35° < \alpha < 37°$ are important consequences of vortex burst, which modifies the dynamic stability of the rolling system [4].
Furthermore, the variability of the oscillation amplitude $\sigma_{\%}$ is larger for $\alpha > 37°$ due to the natural unsteadiness of vortex breakdown locations

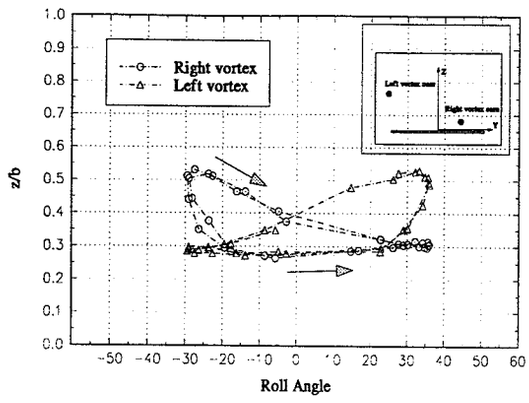

Figure 5: The vortex core displacement (normal axis) in dynamic conditions ($\alpha = 32.5°$).

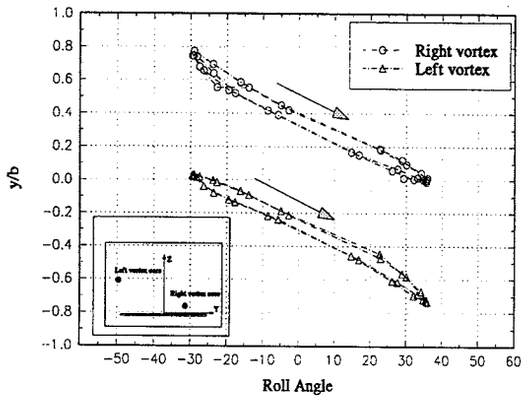

Figure 6: The vortex core displacement (lateral axis) in dynamic conditions ($\alpha = 32.5°$).

($\sigma_{\%} = 6\%$ at $\alpha = 32°$ and $\sigma_{\%} = 20\%$ at $\alpha = 37°$).

Mathematical Modeling

The phase plane representation of the wing rock oscillations (Fig. 15) shows that the phenomenon is dominated by nonlinear damping and a relationship can be established with the analytical models of some single degree of freedom limit cycle oscillators (Duffing's and Van der Pol's equations). The shape of the orbits is elliptic, reflecting the existence of a family of almost sinusoidal solutions:

$$\phi(t) = a(t) \cos(\omega_n t + b(t)) \quad (2)$$

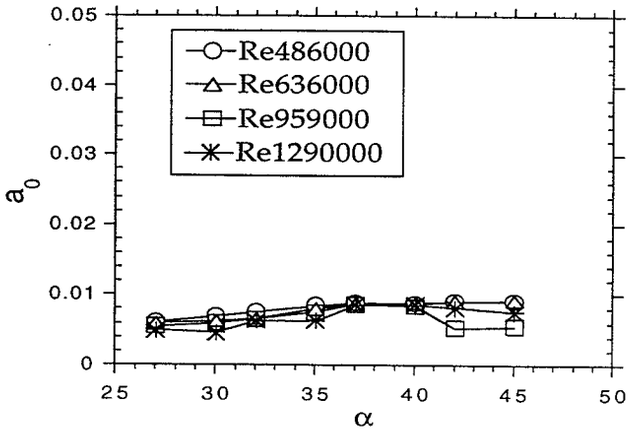

Figure 7: The coefficient a_0 in the analytical model.

where a(t) is the amplitude and b(t) is the phase. Anyway, during the initial cycles of motion, the trajectories with larger amplitudes deform from the purely elliptical shape. This behavior is often seen in dynamical systems which contain a nonlinear restoring moment.

The experimental analysis of the roll attractor [11] demonstrates that the limit cycle is not dependent on the initial condition ϕ_o and the same stable orbits are found with both internal and external release roll angles.

Different analytical nonlinear models were considered in Ref. [11] and the following best fit formulation was identified:

$$\ddot{\phi} + a_0\phi + a_1\dot{\phi} + a_2|\dot{\phi}|\dot{\phi} + a_3\phi^3 + a_4\phi^2\dot{\phi} = 0 \quad (3)$$

where the time derivatives are non dimensional.

The parameters a_i (Fig. 7 - 8 - 9 - 10 - 11) were identified by means of least squares approximation of the experimental results.
The influence of airspeed on these coefficients is evident for a_1, a_2 and a_4 in the α region where vortex burst occurs. As a matter of fact, the combined effect of roll rate and airspeed (i.e. the increase/decrease of $\hat{p} = \dot{\phi}b/2V$) alters the damping generated by the presence of vortex breakdown. The consequence is that limit cycle characteristics are fairly constant with airspeed while build-up dynamics (transient phase) is modified by this damping increase.

Differently, stiffness terms a_0 and a_3 are moderately affected by V (i.e. wing rock natural reduced frequency is substantially unchanged by the

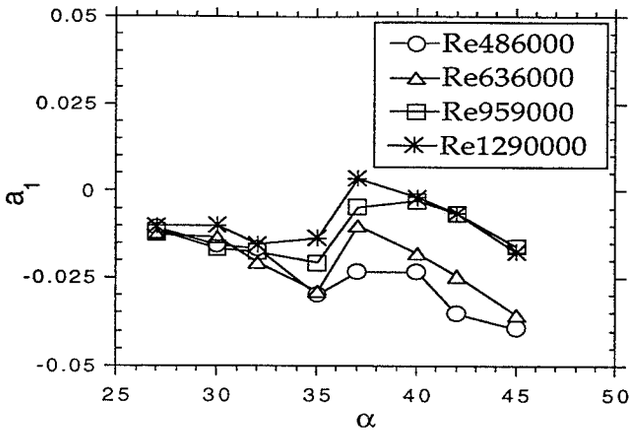

Figure 8: The coefficient a_1 in the analytical model.

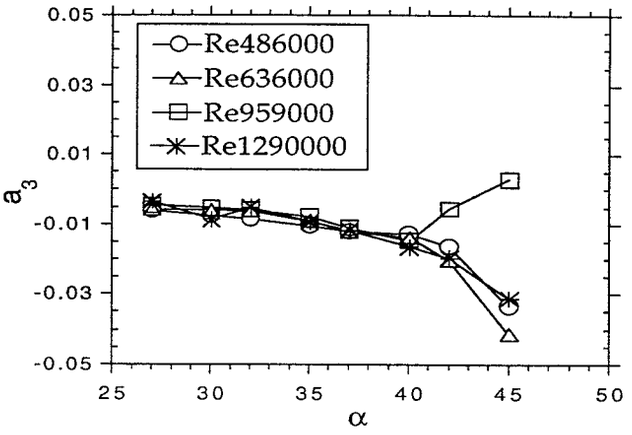

Figure 10: The coefficient a_3 in the analytical model.

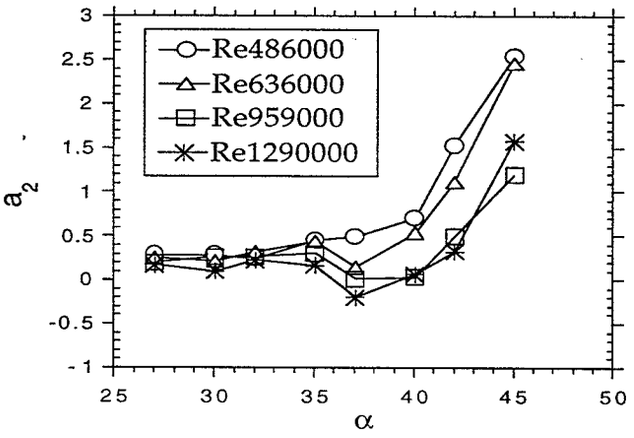

Figure 9: The coefficient a_2 in the analytical model.

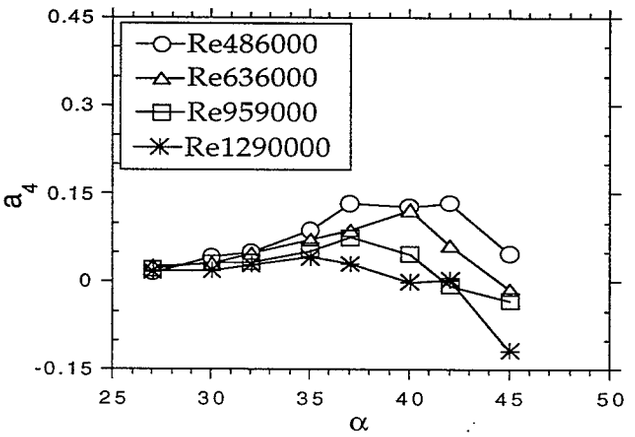

Figure 11: The coefficient a_4 in the analytical model.

increase of airspeed), although a particular divergence from other data is observed for a_3 at high angle of attack at V = 30 m/s (Fig. 10). This result is related to vortex breakdown unsteadiness, typically observed for this wing in the α range over 37°.

Anyway, the minimal changes of the stiffness coefficients produce moderate increments of limit cycle amplitude $\Delta\phi$ with airspeed [11].

The restoring moment $a_0\phi + a_3\phi^3$ (Fig. 12) exhibits a typical trend with softening of linear stiffness a_0. As a consequence the system is statically divergent for $\phi > \sqrt{-a_0/a_3}$.

The reduced order model

$$\ddot{\phi} + a_0\phi + a_3\phi^3 = 0 \qquad (4)$$

describes an undamped system with nonlinear stiffness.

Assuming that $\phi(\hat{t}) = \Delta\phi \sin k\hat{t}$, the locus of solutions (Fig. 14) is given by the values $(\Delta\phi, k)$ that respect the following equation:

$$1 - \frac{k^2}{a_0} + \frac{3}{4} \cdot \frac{a_3}{a_0} \Delta\phi^2 = 0 \qquad (5)$$

The damping coefficient $(a_1 + a_4\phi^2)$ is nonlinear and negative for $\phi < \sqrt{-a_1/a_4}$ (Fig. 13). The system is dynamically unstable for lower roll angles becoming stable as ϕ increases up to the inversion point. The coordinate for this dynamic stability

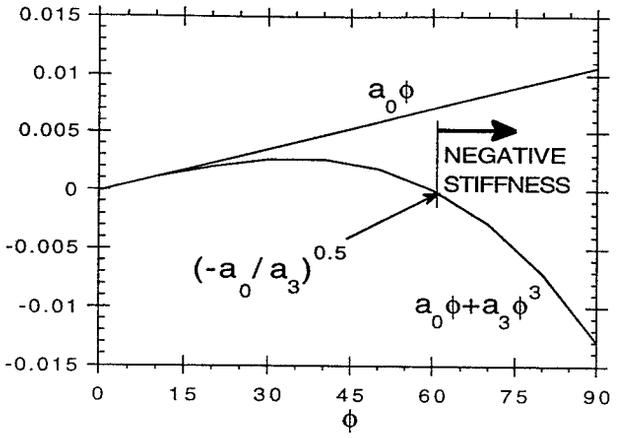

Figure 12: The effect of roll angle on restoring moment in the analytical model ($\alpha = 32.5°$).

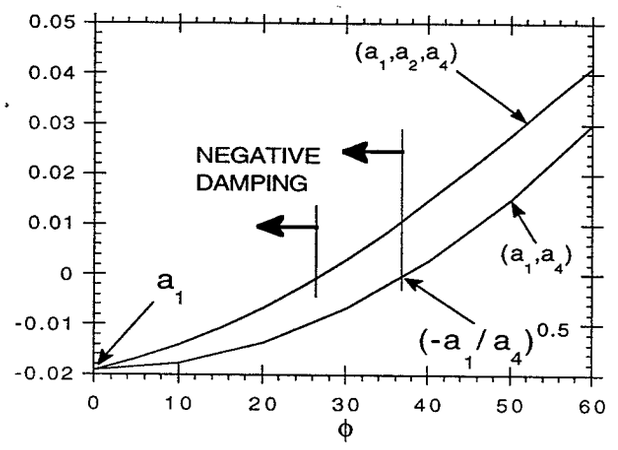

Figure 13: The nonlinear effect of roll angle on damping term in the analytical model ($\alpha = 32.5°$).

cross-over is not coincident with limit cycle amplitude, as the stability of final state occurs when

$$E = qSb \oint_\ell C_l(\phi)\, d\phi = 0 \qquad (6)$$

This condition is required for the balance between dissipation and generation of energy and for a stable oscillatory limit cycle.

Dynamic stability and limit cycle characteristics are also influenced by the additional damping produced by the term $a_2|\dot{\phi}|$.
An equivalent linear damping can be derived if the limit cycle is represented by the function $\phi(\hat{t}) = \Delta\phi \sin k\hat{t}$. The equivalence is established assuming that the dissipation of energy over a complete cycle is the same ($T = 2\pi/k$):

$$\begin{aligned} E_d &= 4\int_0^{T/4} a_n|\dot{\phi}|^n\, d\phi \\ &= 4\int_0^{T/4} a_n|\dot{\phi}|^{n+1}\, d\hat{t} \\ &= 4\, a_n\, k^n\, \Delta\phi^{n+1} \int_0^{\pi/2} |\cos k\hat{t}|^{n+1}\, dk\hat{t} \\ &= \pi\, a_n\, k^n\, \Delta\phi^{n+1}\gamma_n \end{aligned}$$

where

$$\gamma_n = \frac{4}{\pi}\int_0^{\pi/2} |\cos k\hat{t}|^{n+1}\, dk\hat{t} \qquad (7)$$

Hence, the equivalent linear damping term a_{eq} is obtained as

$$a_{eq} = a_2\, k\, \Delta\phi \frac{\gamma_2}{\gamma_1} = a_2\, k\, \Delta\phi \frac{8}{3\pi} \qquad (8)$$

This last equation allows to include the damping coefficient $a_{eq} \approx a_2|\dot{\phi}|$ in the nonlinear model (Fig. 13). As a consequence, the cross-over point is shifted to lower roll angles with a stabilizing effect.

The locus of solutions $(\Delta\phi, k)$ that respect

$$E_d = \oint_\ell (a_1 + a_2|\dot{\phi}| + a_4\phi^2)\, \dot{\phi}\, d\phi = 0 \qquad (9)$$

is also compared in Fig. 14 with the solutions for the undamped system. The stable limit cycle is quite accurately estimated by the intersection of the two plots for eqns. 5 and 9. Overprediction of frequency

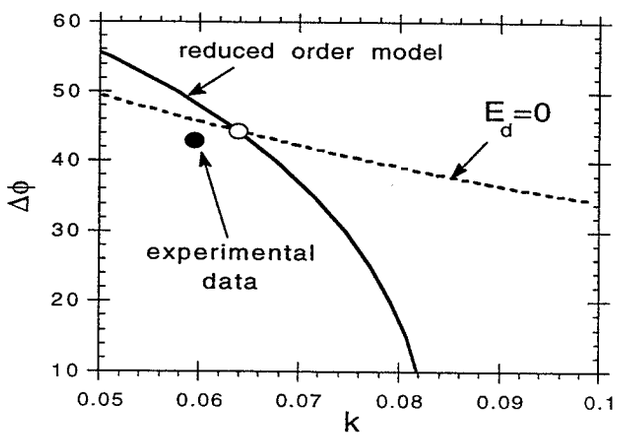

Figure 14: Comparison of experimental results with a reduced order analytical model ($\alpha = 32.5°$).

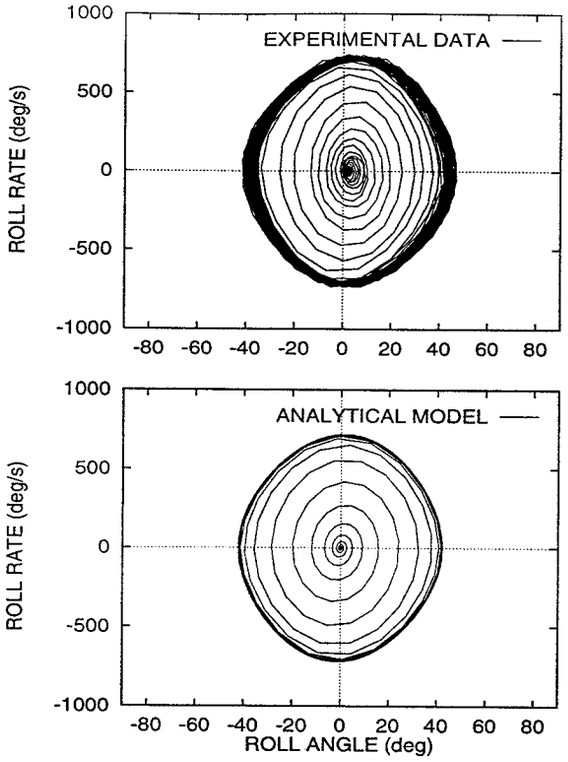

Figure 15: Comparison of experimental and analytical phase plane plots ($\alpha = 32.5^o - \phi_o \approx 0$).

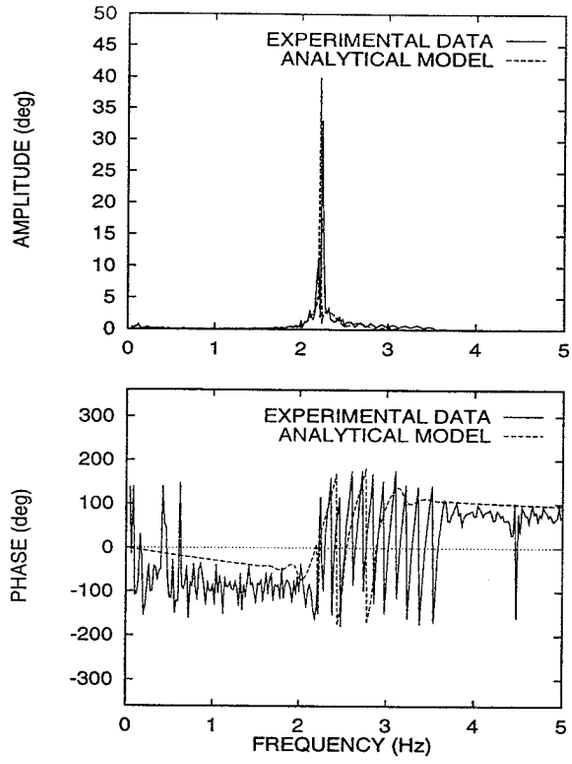

Figure 16: Comparison of experimental and analytical spectral data ($\alpha = 32.5^o$ - Re = 636000).

and amplitude is related with the approximation introduced in the reduced order system (decoupling of restoring and damping moments).

Model Validation

Time domain validations were performed by comparing numerical integrations of the mathematical model with experimental data (Fig. 15).
The prediction of the wing rock oscillations is always accurate for $\phi_o < \Delta\varphi$. On the contrary an unexpected divergence is found for external initial conditions ($\phi_o > 60°$).
The discrepancy between experiments and analytical approximations is explained considering that the model includes a cubic softening term. Previous studies [10] proved that the importance of this contribution is related with the divergence of the motion starting with peculiar initial conditions, such as large ϕ_o. Hence, a correct mathematical model should include a cubic parameter $a_3(\alpha, \phi_o)$ evaluated from experimental data with different release roll angles. This model improvement has no practical impact taking into account that the onset of in-flight wing rock is triggered for moderate aircraft initial roll angles ϕ_o.

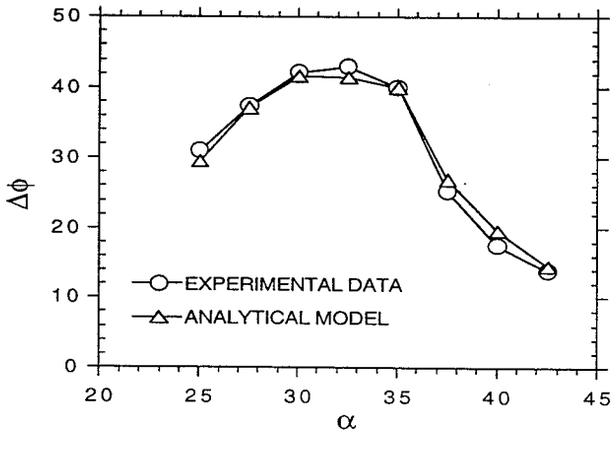

Figure 17: Comparison of experimental and analytical limit cycle amplitude (Re = 636000).

Frequency domain validation (Fig. 16) also confirms the accurate reproduction of the spectral components of time histories ϕ(t) during the stable oscillatory phase. Differently, an approximate reconstruction of build-up frequencies is obtained by the analytical model, that smoothes the frequency stretching clearly observed in the very initial phase

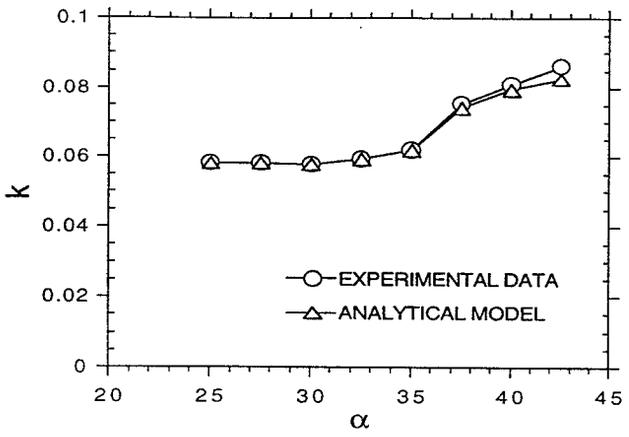

Figure 18: Comparison of experimental and analytical limit cycle frequency (Re = 636000).

of the experimental measurements (clustering of roll trajectories in Fig. 15).

Complete numerical simulations show that overall limit cycle characteristics are correctly reproduced by the analytical model (Fig. 17 - 18).

Concluding Remarks

Free-to-roll experiments were performed on a 80° delta wing undergoing self induced wing rock oscillations. The tests were carried out at different angles of attack, airspeeds and initial roll angles in order to investigate the influence of the experimental parameters on the limit cycle.

The amplitude of the oscillatory mode is a nonlinear function of incidence and its maximum is reached at $\alpha = 32.5°$. Stable limit cycles were observed for $\alpha \geq 25°$. The progressive reduction of angle of attack during the self sustained oscillations suppressed the wing rock motion at $\alpha < 25°$.

The comparison with other reference experimental data confirms that the measurements performed at TPI are accurate.

The oscillatory behavior was reproduced by an analytical model, based on a parametric analysis of the experimental results. The model was validated (time domain and frequency domain validation). The nonlinear contributions of coefficients in the mathematical model were discussed.

References

[1] Hsu, C.H., Lan, C.E., *Theory of Wing Rock* , J. of Aircraft, vol. 22, no. 10, p. 920-924, 1985.

[2] Levin, D., Katz, J., *Dynamic Load Measurements with Delta Wings Undergoing Self Induced Roll Oscillations* , J. of Aircraft, vol. 21, no. 1, p. 30-36, 1984.

[3] Nguyen, L.T., Yip, L.P., Chambers, J.R., *Self Induced Wing Rock of Slender Delta Wings* , AIAA Atmospheric Flight Mechanics Conference, Albuquerque, USA, 1981.

[4] Arena, Jr., A.S., *An Experimental and Computational Investigation of Slender Wings Undergoing Wing Rock* , PhD Dissertation, University of Notre Dame, Indiana, USA, 1992.

[5] Arena, Jr., A.S., Nelson, R.C., *An Experimental Study of the Nonlinear Dynamic Phenomenon Known as Wing Rock* , AIAA no. 90-2812, 1990.

[6] Arena, Jr., A.S., Nelson, R.C., *Measurement of Unsteady Surface Pressure on a Slender Wing Undergoing a Self Induced Oscillation* , Exp. in Fluids, vol. 16, no. 6, p. 414-416, 1994.

[7] Yoshinaga, T., Tate, A., Noda, J., *Wing Rock of Delta Wings with an Analysis by the Phase Plane Method* , AIAA Atmospheric Flight Mechanics Conference, Monterey, USA, 1993.

[8] Quast, T., Nelson, R.C., Fisher, D.F., *A Study of High Alpha Dynamics and Flow Visualization for a 2.5% Model of the F-18 HARV Undergoing Wing Rock* , AIAA Applied Aerodynamics Conference, Baltimore, USA, 1991.

[9] Quast, T., *A Study of High Alpha Dynamics and Flow Visualization for a 2.5% Model of the F-18 HARV Undergoing Wing Rock* , MS Thesis, University of Notre Dame, Indiana, USA, 1991.

[10] Nayfeh, A.H., Elzebda, J.M., Mook D.T., *Analytical Study of the Subsonic Wing Rock Phenomenon for Slender Delta Wings* , J. of Aircraft, vol. 26, no. 9, p. 805-809, 1989.

[11] Guglieri, Quagliotti, F.B., *Experimental Observation and Discussion of the Wing Rock Phenomenon*, Aerospace Science and Technology, vol. 1, no. 2, 1997